Molecular Imaging
Volume 16 : 1-5
© The Author(s) 2017
Reprints and permission:
sagepub.com/journalsPermissions.nav
DOI: 10.1177/1536012117718459
journals.sagepub.com/home/mix
SAGE

Noninvasive Imaging of Immune Checkpoint Ligand PD-L1 in Tumors and Metastases for Guiding Immunotherapy

Samit Chatterjee, PhD[1], Wojciech G. Lesniak, PhD[1], and Sridhar Nimmagadda, PhD[1,2]

Abstract

Immunotherapy holds great promise in cancer treatment. The challenges in advancing immunotherapies lie in patient stratification and monitoring therapy. Noninvasive detection of immune checkpoint ligand PD-L1 can serve as an important biomarker for guidance and monitoring of immunotherapy. Here in, we provide an overview of our efforts to develop clinically translatable PD-L1-specific imaging agents for quantitative and real-time assessment of PD-L1 expression in tumor microenvironment.

Keywords

immunotherapy, PET, SPECT, optical imaging, atezolizumab, peptide, PD-1

Immunotherapy is emerging as an important treatment modality for various cancers.[1] Using this approach, cancer is treated by augmenting or generating an immune response against tumor cells. Tumor cells escape from immune response by deploying immunosuppressive mechanisms such as immune checkpoints.[2] These ligand–receptor interaction-mediated checkpoints modulate the amplitude and duration of immune response and act as a natural "brake" of the immune system to maintain self-tolerance. Targeting and modulating the immune checkpoint proteins by antibodies has become a powerful therapeutic strategy for anticancer immunotherapy. A major therapeutic target is the immune checkpoint axis of programmed death receptor 1 (PD-1 and CD279) and its ligand PD-L1 (B7-H1 and CD274). In a number of cancers including melanoma, renal cell carcinoma (RCC), lung, breast, ovarian, and colorectal cancers, PD-L1 expression has been shown to be upregulated constitutively[3] or due to inflammation in the tumor microenvironment (TME), leading to deactivation of PD-1-expressing tumor-infiltrating lymphocytes (TILs) that results in immune suppression.[2]

Cancer treatments targeting immune checkpoints have shown robust and durable clinical responses that lead to long-term survival in some patients.[2] Several immune checkpoint targeting antibody therapeutics have received Food and Drug Administration approval. PD-L1 targeting antibodies such as MPDL3280A (atezolizumab), MEDI4736 (durvalumab), and Avelumab have demonstrated anticancer activity in multiple tumor types including advanced melanoma,[4] non-small-cell lung cancer (NSCLC),[5] RCC,[6] and bladder cancer.[7] Nearly 70% of patients with cancer do not respond to checkpoint blockade therapies, however. There is a pressing clinical need to accurately predict which patients are more likely to benefit from immunotherapy.

Methods of monitoring conventional cancer therapy can be confounding to measure immunotherapy response. For example, tumor shrinkage is initially observed in only $\sim$10% patients with immunotherapy but is a typical positive response with cytotoxic therapy. Delayed response to therapy following initial increase in tumor burden is also observed in some patients, indicative of immune-mediated response. Concurrently, it is known from biopsy specimens of tumors

[1] Russell H. Morgan Department of Radiology and Radiological Science, Johns Hopkins Medical Institutions, Johns Hopkins University, Baltimore, MD, USA
[2] Sidney Kimmel Comprehensive Cancer Center, Johns Hopkins University, Baltimore, MD, USA

Submitted: 26/05/2017. Revised: 04/06/2017. Accepted: 04/06/2017.

Corresponding Author:
Sridhar Nimmagadda, Russell H. Morgan Department of Radiology and Radiological Science, Johns Hopkins Medical Institutions, Johns Hopkins University, 1550 Orleans Street, CRB II, #491, Baltimore, MD 21287, USA.
Email: snimmag1@jhmi.edu

from patients undergoing immune checkpoint therapy that PD-L1 expression within the TME is relevant to achievement of response.[8]

Currently, PD-L1 expression in the tumors is evaluated by immunohistochemistry (IHC). Food and Drug Administration has recently approved 2 IHC companion diagnostic tests (PD-L1 IHC 22C3 pharmDx and PD-L1 IHC 28-8 pharmDx). However, PD-L1 IHC has considerable inadequacies such as variable criteria for quantification, different antibodies for detection, variability in tissue preparation and processing, and heterogeneity of PD-L1 expression in primary tumors and in metastatic lesions. Also, it is impractical to perform repeated biopsy to monitor therapy response. Moreover, these limitations are compounded in patients with advanced stage disease. Thus, we hypothesized that noninvasive imaging could be a complementary and superior tool to determine in vivo PD-L1 expression in all the lesions in entirety, providing more accurate assessment of PD-L1 for therapy management.

For noninvasive detection of PD-L1, we chose atezolizumab from Genentech (San Francisco, CA) due to its extensive clinical use in cancer immunotherapy. Atezolizumab is an effector function deficient humanized immunoglobulin G1 (IgG1) monoclonal antibody with impaired binding to Fcγ receptor that minimizes depletion of PD-L1-positive tumor-specific T cells. Atezolizumab has high binding affinity toward human (dissociation constant $K_d = 0.43$ nM) and mouse PD-L1 ($K_d = 0.13$ nM),[7,9] thus providing an opportunity to relate preclinical and clinical observations.

To begin with, we developed atezolizumab radiolabeled with indium 111 ([^{111}In]atezolizumab) and conjugated with Licor 800 near-infrared dye (NIR-atezolizumab) for evaluation of PD-L1 expression. The binding specificity of [^{111}In]atezolizumab and NIR-atezolizumab to PD-L1 was first validated in vitro in multiple cell lines with varying levels of PD-L1 expression. Significantly higher uptake of [^{111}In]atezolizumab and NIR-atezolizumab was observed in cell lines with high PD-L1 expression. In vivo assessment of [^{111}In]atezolizumab binding to tumor PD-L1 was carried out by single-photon emission computed tomography/computed tomography (SPECT/CT) imaging in immunocompromised non-obese diabetic severe-combined immunodeficient gamma (NSG) mice bearing transfected Chinese hamster ovary (CHO) tumor with high PD-L1 expression (hPD-L1 tumor) and control CHO tumor. SPECT/CT imaging showed significantly higher accumulation of [^{111}In]atezolizumab in hPD-L1 tumor compared to control CHO tumor, confirming in vivo binding specificity of [^{111}In]atezolizumab to PD-L1 (Figure 1A). We further validated [^{111}In]atezolizumab in xenograft models with clinically relevant PD-L1 expression levels. Specificity of [^{111}In]atezolizumab was confirmed in orthotopic triple negative breast cancer (TNBC) (MDAMB231 PD-L1 high and SUM149 PD-L1 low) and NSCLC (H2444 PD-L1 high and H1155 PD-L1 low) xenografts expressing varying levels of PD-L1. Differential accumulation of NIR-atezolizumab in tumors was also observed in the same xenograft models in optical imaging studies. Collectively, those findings demonstrated the feasibility of noninvasive SPECT/CT and optical imaging of tumor PD-L1 expression using atezolizumab (Figure 1A and C).[10]

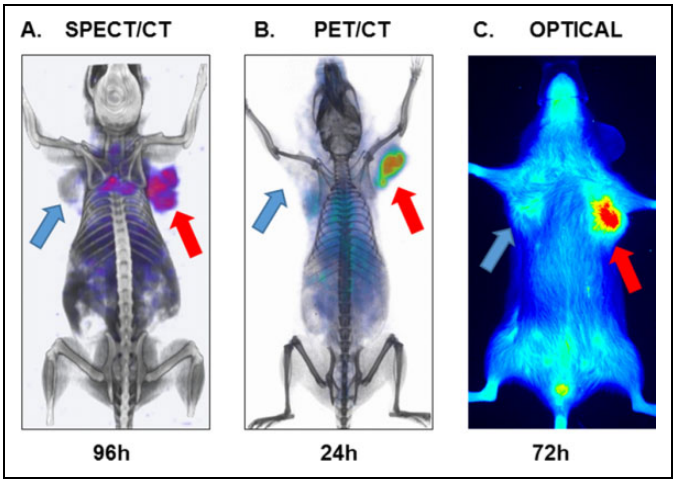

Figure 1. Imaging of tumor PD-L1 using atezolizumab: (A) SPECT/CT, (B) PET/CT, and (C) NIR imaging of PD-L1 using [^{111}In]atezolizumab, [^{64}Cu]atezolizumab, and NIR-atezolizumab, respectively, in NSG mice-bearing hPD-L1 tumor (red arrow) and control CHO (blue arrow) tumors. Adapted from Chatterjee et al[10] and Lesniak et al[11]. CT indicates computed tomography; CHO, Chinese hamster ovary; PET, positron emission tomography; NIR, near-infrared; NSG, non-obese diabetic severe-combined immunodeficient gamma; SPECT, single-photon emission computed tomography.

Encouraged by those results, we pursued the development of a PD-L1-targeting positron emission tomography (PET) imaging agent. PET is one of the most sensitive high-resolution imaging technologies used for quantitative imaging of target expression in tumors. PET imaging agents providing real-time quantitation of target expression relevant to immunotherapy can be useful for guiding and monitoring therapy. To develop PD-L1-targeting PET tracer, we conjugated atezolizumab with 2,2′,2″-(10-(2,6-dioxotetrahydro-2*H*-pyran-3-yl)-1,4,7,10-tetraazacyclododecane-1,4,7-triyl)triacetic acid (DOTAGA anhydrate), and radiolabeled with copper-64 to prepare [^{64}Cu]atezolizumab.[11] The PD-L1 specificity of [^{64}Cu]atezolizumab was assessed in vitro in multiple cell lines with varying PD-L1 expression which demonstrated a strong correlation ($R = .997$) between [^{64}Cu]atezolizumab uptake and PD-L1 expression. Next, we performed PET/CT imaging in NSG mice with hPD-L1 and control CHO tumors which evidently demonstrated increased uptake of [^{64}Cu]atezolizumab in hPD-L1 tumor compared to the control tumor (Figure 1B). Further the specificity of [^{64}Cu]atezolizumab was confirmed in orthotopic MDAMB231 and SUM149 TNBC tumor models with high and low PD-L1 expression, respectively. Uptake of [^{64}Cu]atezolizumab in MDAMB231 tumor was significantly higher than SUM149 tumor, validating the potential of [^{64}Cu]atezolizumab to differentiate clinically relevant expression levels of PD-L1. Since atezolizumab is cross-reactive to human and mouse PD-L1, we took advantage of this dual affinity to evaluate tumor PD-L1 in the presence of an active immune

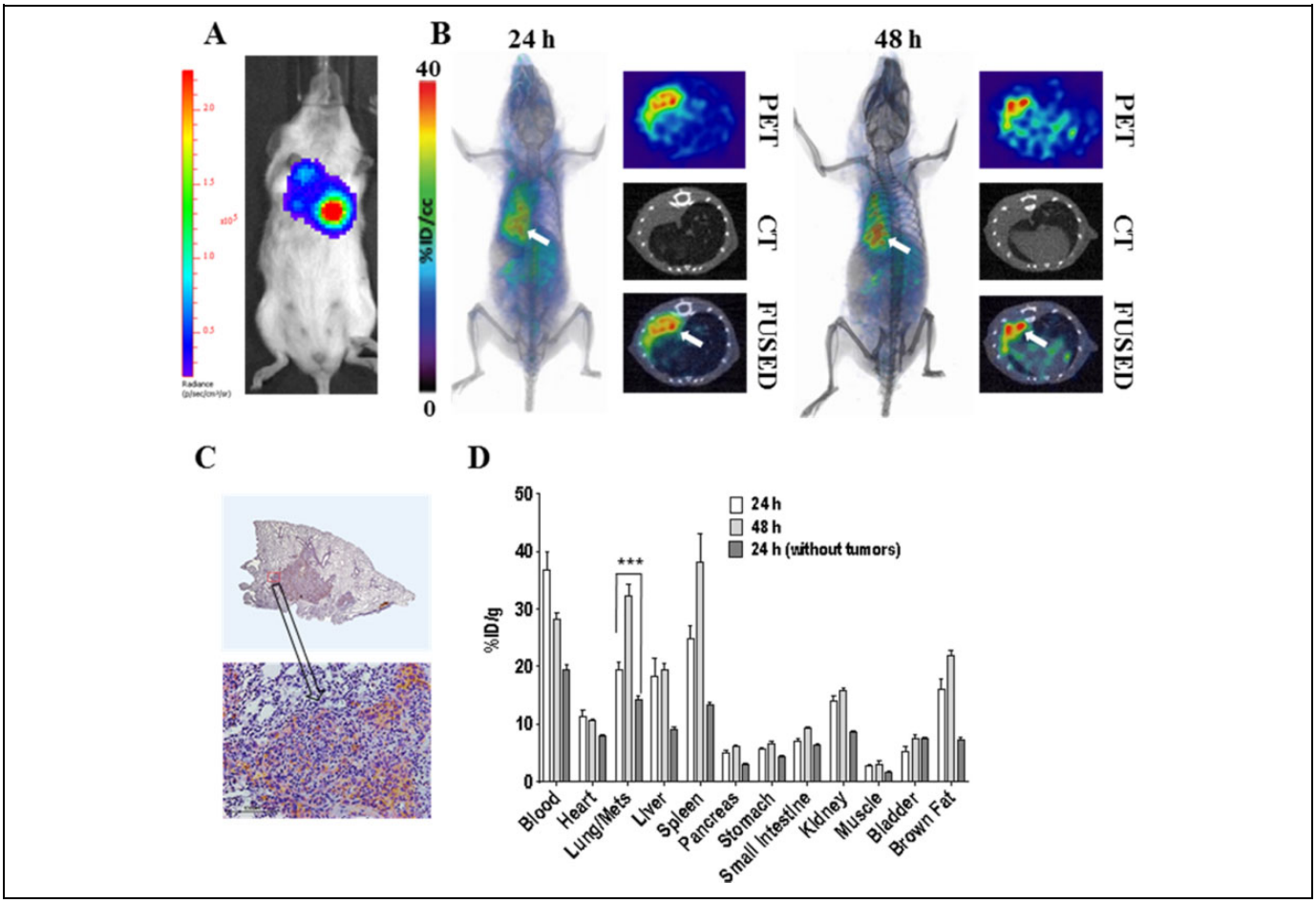

Figure 2. Evaluation of [^{64}Cu]atezolizumab in MDAMB231-luc-derived lung metastases. To generate tumors mimicking lung metastases, MDAMB231-luc cells (1×10^6 in 30 μL HBSS with 50% Matrigel) were injected into the left lung of NSG mice. Growth of tumors was monitored by bioluminescent imaging after injection of luciferin and mice were used for experiments 28 days after inoculation. (A) Representative bioluminescence image of a mouse indicating the formation of the MDAMB231-luc lung metastases; (B) volume rendered (left panel) and transaxial (right panel) PET-CT images confirming high accumulation of radioactivity in lung metastases (white arrows; n = 3); (C) IHC analysis of PD-L1 expression demonstrating intense immunoreactivity in MDAMB231-luc lung metastases. (D) Ex vivo biodistribution analysis of the [^{64}Cu]atezolizumab at 24- and 48-hour PI, in the same metastases model and in mice without lung metastases (n = 4); P <.001; *** (n = 4). CT indicates computed tomography; HBSS, Hank's balanced salt solution; IHC, immunohistochemistry; NSG, non-obese diabetic severe-combined immunodeficient gamma; PET, positron emission tomography.

system, parts of which also express PD-L1. PET and biodistribution of [^{64}Cu]atezolizumab was performed in immunocompetent Balb/C mice harboring the syngeneic 4T1 mouse mammary carcinoma expressing mouse PD-L1. PET imaging demonstrated high and persistent uptake of [^{64}Cu]atezolizumab in 4T1 tumors. Radioactivity was also detected in tissues with known endogenous PD-L1 expression such as lymph nodes, liver, brown adipose tissue, and spleen, with 4T1 tumors showing much higher uptake of [^{64}Cu]atezolizumab than those tissues. Since PD-L1-positive TILs may also partially contribute to the uptake of [^{64}Cu]atezolizumab in the TME, we quantified the amount of TILs. Ex vivo analysis of 4T1 tumor cell suspension by flow cytometry revealed that only minor proportion (~6%) of TILs is PD-L1 positive, indicating that [^{64}Cu]atezolizumab accumulation in the TME was mostly associated with PD-L1 expression on 4T1 tumor cells.

Apart from the above described published studies conducted in primary tumors, we also tested the feasibility of PD-L1 PET with [^{64}Cu]atezolizumab in a breast cancer lung metastasis model. To mimic the discrete lung metastases observed with breast cancers, we injected MDAMB231 cells that stably expressed firefly luciferase (MDAMB231-luc) into lungs and used [^{64}Cu]atezolizumab to detect PD-L1 expression in the metastatic lesions (Figure 2). As demonstrated in Figure 2A, formation of the lung metastases was confirmed with bioluminescence imaging. Following PET-CT studies indicated high accumulation of radioactivity in lung metastases 24 and 48 hours after injection of [^{64}Cu]atezolizumab (Figure 2B), which allowed for clear delineation of the tumors from normal lung tissue. High uptake of [^{64}Cu]atezolizumab in lung metastases was validated by intense PD-L1 staining in IHC as presented in

Figure 2C. To further endorse PET-CT imaging results, we performed head-to-head comparative ex vivo biodistribution analysis of [^{64}Cu]atezolizumab in mice-bearing MDA-MB-321-luc lung metastases and in healthy mice without lung metastases (Figure 2D). There was notably higher accumulation of [^{64}Cu]atezolizumab in lungs with MDAMB231-luc metastases (19.72 $\pm$ 3.1%ID/g at 24 hours post injection [PI] and 32.1 $\pm$ 3.7%ID/g at 48 hours PI) compared to lungs without tumors (14.2 $\pm$ 3.1%ID/g at 24 hours PI and 11.4 $\pm$ 1.2%ID/g at 48 hours PI).

Taken together, our studies in different tumor models with variable PD-L1 expression in immunocompromised or immunocompetent mice, and in a metastatic model demonstrated the potential of [^{64}Cu]atezolizumab PET for noninvasive detection of PD-L1 in tumors and metastases. Biodistribution of this human and mouse cross-reactive antibody is also complementary to the reports by other groups on PD-L1 imaging using murine PD-L1-reactive antibodies.[12-14,15] One of the interesting observations is the antibody uptake in brown fat, an immunologically relevant tissue, in preclinical models.

Atezolizumab is in different phases of clinical trials for the treatment of NSCLC (NCT03014648, NCT02848651, and NCT02927301), advanced or metastatic urothelial bladder cancer (NCT02951767, NCT02108652), gynecological cancers (NCT03073525), Hodgkin lymphoma (NCT03120676), colorectal cancer (NCT02982694), TNBC (NCT03125902), prostate cancer (NCT02814669), nonclear cell kidney cancer (NCT02724878), and RCC (NCT03024996). [^{89}Zr]Atezolizumab imaging in patients showed heterogeneous uptake in tumors between and within patients validating preclinical observations (NCT02453984).[16]

Despite increased use of radiolabeled antibodies for imaging tumor-specific biomarkers, desired image contrast and sensitivity require longer clearance times often extending up to days which is impractical for routine clinical use. This prompted us to develop a PET imaging agent that can rapidly detect PD-L1 to capture the dynamic changes in PD-L1 expression in the TME. For this purpose, low-molecular-weight peptide-based PET tracers are preferred candidates for clinical applications due to faster clearance and synthetic tractability. PD-L1 binding peptides have recently been reported,[17] although potential of those peptides to detect PD-L1 expression in vivo has not been demonstrated. We selected the peptide WL12 (or 1246)[17] that possessed high binding affinity to PD-L1 and has an ornithine residue that could be selectively modified to obtain a radiotracer while retaining affinity to PD-L1.[18] A DOTAGA chelator was conjugated to the peptide and radiolabeled with copper-64 to form [^{64}Cu]WL12. The specificity of [^{64}Cu]WL12 binding to PD-L1 was assessed in vitro in multiple cell lines with variable PD-L1 expression by performing binding assay which showed a correlation between [^{64}Cu]WL12 uptake and PD-L1 expression. In proof-of-concept studies, we validated [^{64}Cu]WL12 as a PD-L1-specific PET tracer in NSG mice with hPD-L1 tumors and control CHO tumors. PET imaging and biodistribution studies showed that

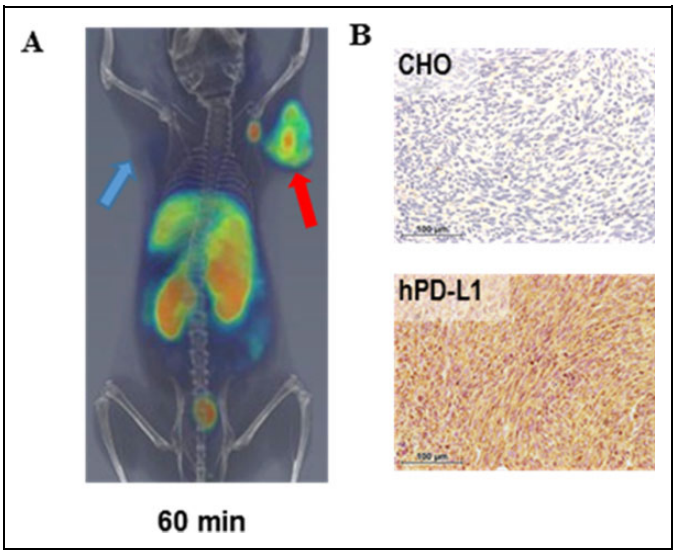

Figure 3. Rapid detection of tumor PD-L1 by [^{64}Cu]WL12 PET: (A) PET/CT imaging of PD-L1 using [^{64}Cu]WL12 in NSG mice-bearing hPD-L1 (red arrow) and control CHO (blue arrow) tumors at 60-minute PI; (B) PD-L1 IHC staining in CHO and hPD-L1 tumor sections. Adapted from Chatterjee et al.[18] CT indicates computed tomography; CHO, Chinese hamster ovary; IHC, immunohistochemistry; NSG, non-obese diabetic severe-combined immunodeficient gamma; PET, positron emission tomography.

[^{64}Cu]WL12 is capable of detecting PD-L1 expression within an hour after injection. [^{64}Cu]WL12 accumulation was significantly higher in hPD-L1 than in control CHO tumors (Figure 3). This rapid and specific detection of tumor PD-L1 expression by [^{64}Cu]WL12 PET fits well within the clinical work flow of imaging within 60 minutes of tracer administration.

In summary, we developed PD-L1-specific nuclear and optical imaging agents using a clinically relevant therapeutic antibody. We also developed a peptide-based PET imaging agent with improved sensitivity for rapid detection of PD-L1 in tumors. Rapid and noninvasive detection of PD-L1 expression in various cancers could potentially aid in therapy guidance. These developments create the opportunity to utilize imaging biomarker-driven approaches of patient management and appropriate modulation of immunotherapy to achieve best clinical outcomes.

Declaration of Conflicting Interests

The author(s) declared no potential conflicts of interest with respect to the research, authorship, and/or publication of this article.

Funding

The author(s) disclosed receipt of the following financial support for the research, authorship, and/or publication of this article: Funding for this study was provided by Allegheny Health Network-Johns Hopkins Cancer Research Fund (SN) and NIHR01CA16631 (SN). Flow cytometry, histology, and imaging resources were supported by NIHP30 CA006973.

References

1. Topalian SL, Taube JM, Anders RA, Pardoll DM. Mechanism-driven biomarkers to guide immune checkpoint blockade in cancer therapy. *Nat Rev Cancer*. 2016;16(5):275–287.
2. Topalian SL, Drake CG, Pardoll DM. Immune checkpoint blockade: a common denominator approach to cancer therapy. *Cancer Cell*. 2015;27(4):450–461.
3. Parsa AT, Waldron JS, Panner A, et al. Loss of tumor suppressor PTEN function increases B7-H1 expression and immunoresistance in glioma. *Nat Med*. 2007;13(1):84–88.
4. Hamid O, Sosman JA, Lawrence DP, et al. Clinical activity, safety, and biomarkers of MPDL3280A, an engineered PD-L1 antibody in patients with locally advanced or metastatic melanoma (mM). *J Clin Oncol*. 2013;31(suppl 15): 9010.
5. Spigel DR, Gettinger SN, Horn L, et al. Clinical activity, safety, and biomarkers of MPDL3280A, an engineered PD-L1 antibody in patients with locally advanced or metastatic non-small cell lung cancer (NSCLC). *J Clin Oncol*. 2013;31:abstr 8008.
6. Cho DC, Sosman JA, Sznol M, et al. Clinical activity, safety, and biomarkers of MPDL3280A, an engineered PD-L1 antibody in patients with metastatic renal cell carcinoma (mRCC). *J Clin Oncol*. 2013;31(15_suppl):4505–4505.
7. Powles T, Eder JP, Fine GD, et al. MPDL3280A (anti-PD-L1) treatment leads to clinical activity in metastatic bladder cancer. *Nature*. 2014;515(7528):558–562.
8. Herbst RS, Soria JC, Kowanetz M, et al. Predictive correlates of response to the anti-PD-L1 antibody MPDL3280A in cancer patients. *Nature*. 2014;515(7528):563–567.
9. Irving B, Chiu H, Maecker H, et al. *Anti-PD-L1 Antibodies, Compositions and Articles of Manufacture*. In: Office (Patent US8217149, www.google.com/patents/US8217149), ed. San Francisco, CA, USA: Genentech, Inc.; 2012.
10. Chatterjee S, Lesniak WG, Gabrielson M, et al. A humanized antibody for imaging immune checkpoint ligand PD-L1 expression in tumors. *Oncotarget*. 2016;7(9):10215–10227.
11. Lesniak WG, Chatterjee S, Gabrielson M, et al. PD-L1 detection in tumors using [(64)Cu]atezolizumab with PET. *Bioconjug Chem*. 2016;27(9):2103–2110.
12. Heskamp S, Hobo W, Molkenboer-Kuenen JD, et al. Noninvasive imaging of tumor PD-L1 expression using radiolabeled anti-PD-L1 antibodies. *Cancer Res*. 2015;75(14):2928–2936.
13. Hettich M, Braun F, Bartholoma MD, Schirmbeck R, Niedermann G. High-resolution PET imaging with therapeutic antibody-based PD-1/PD-L1 checkpoint tracers. *Theranostics*. 2016;6(10): 1629–1640.
14. Josefsson A, Nedrow JR, Park S, et al. Imaging, biodistribution, and dosimetry of radionuclide-labeled PD-L1 antibody in an immunocompetent mouse model of breast cancer. *Cancer Res*. 2016;76(2):472–479.
15. Deng R, Bumbaca D, Pastuskovas CV, et al. MAbs. 2016;8(3): 593–603. doi: 10.1080/19420862.2015.1136043. Epub 2016 Feb 26.
16. Bensch F, Veen E, Jorritsma A, et al. First-in-human PET imaging with the PD-L1 antibody 89Zr-atezolizumab. Paper presented at: AACR Annual Meeting, Washington Convention Center, April 2, 2017. CT017.
17. Miller MM, Mapelli C, Allen MP, et al. *Macrocyclic Inhibitors of the pd-1/pd-l1 and cd80 (b7-1)/pd-li Protein/Protein Interactions*. WIPO (WO2014151634), USA: Bristol Myers Squibb Co. 20161093pp, WO2016039749A1; 2016.
18. Chatterjee S, Lesniak WG, Miller MS, et al. Rapid PD-L1 detection in tumors with PET using a highly specific peptide. *Biochem Biophys Res Commun*. 2017;483(1):258–263.